Discordant Pleistocene population size histories in a guild of hymenopteran parasitoids

William Walton[1], Graham N Stone[1], and Konrad Lohse *[1]

[1]Institute of Evolutionary Biology, University of Edinburgh, EH9 3FL, UK

* correspondence to konrad.lohse@ed.ac.uk

Abstract

Signatures of past changes in population size have been detected in genome-wide variation in many species. However, the causes of such demographic changes and the extent to which they are shared across co-distributed species remain poorly understood. During Pleistocene glacial maxima, many temperate European species were confined to southern refugia. While vicariance and range expansion processes associated with glacial cycles have been widely studied, little is known about the demographic history of refugial populations, and the extent and causes of demographic variation among co-distributed species. We used whole genome sequence data to reconstruct and compare demographic histories during the Quaternary for Iberian refuge populations in a single ecological guild (seven species of chalcid parasitoid wasps associated with oak cynipid galls). We find support for large changes in effective population size (N_e) through the Pleistocene that coincide with major climate events. However, there is little evidence that the timing, direction and magnitude of demographic change are shared across species, suggesting that demographic histories are largely idiosyncratic even at the scale of a single glacial refugium.

Keywords: N_e change, comparative phylogeography, glacial refugia, population genomics, chalcid

Introduction

Natural populations change in size and range in response to biotic and abiotic factors over both ecological and evolutionary timescales. Given that sequence variation is the only source of information about the evolutionary past of many taxa, there is considerable interest in using genetic data to reconstruct the demographic

history of populations (see 5, for a recent review). A key question is to what extent past demographic changes have been shaped by climatic events and whether such responses are concordant across co-distributed taxa, or vary with species traits (26; 59; 47).

A major aim of phylogeographic studies has been to understand the origins and determinants of spatial structure in natural populations (3; 26). Systematic comparisons of demographic histories across co-distributed taxa offer the chance to identify shared abiotic triggers of demographic events (6; 24; 26). If divergence and admixture between populations are largely the outcome of shared climatic and geological history, one would expect co-distributed and ecologically similar species to show concordant histories. Concordance in vicariance times has indeed been found by a number of comparative phylogeographic studies (e.g. 32; 59; 71; 68). However, most species are likely to have undergone complex range changes and given that range shifts in response to abiotic factors are likely to depend on multiple traits, assumption of strict temporal concordance seems implausibly simplistic biologically (47).

For example, many temperate plant and animal taxa (including humans) have colonised the Western Palaearctic in a series of westwards range expansions. Overlaid onto this older longitudinal colonisation history is a cyclical history of latitudinal range changes (24; 27). Starting with the onset of major glacial cycles in the mid Pleistocene, the ranges of temperate taxa in Europe were restricted to southern refugia during glacial maxima, primarily in Iberia, Italy and the Balkans (24; 17; 27) and expanded northwards during interglacial periods. As a consequence, modern refugial populations commonly harbour higher genetic diversity than northern populations founded by postglacial range expansion (e.g. 24; 52; 63; 65) (but see 12). While the structuring of genetic diversity by refugia is ubiquitous (25), recent comparative studies of the population and speciation history of European taxa have, perhaps unsurprisingly, ruled out temporal concordance (9; 15).

Bunnefeld et al. (9) used whole genome sequence data to compare the timing of divergence and admixture events between three southern refugial populations across 13 co-distributed species in a tritrophic Western Palaearctic community comprising oak (*Quercus*) host plants, cynipid gall wasp herbivores and chalcid parasitoid natural enemies (61). The latter are obligate specialists of cynipid galls, allowing the guild of parasitoids to be considered in ecological isolation. Many of the component species show broad longitudinal distributions, extending from Iberia in the West to Iran in the East, and all species studied to date are genetically structured into major southern refuge populations (59; 62; 44; 43; 39; 37; 48). Bunnefeld et al. (9) showed that many species in this model community colonised refugia in the Balkans and Iberia primarily through westwards range expansion from an eastern origin one or more glacial cycles in the past. While Bunnefeld

et al. (9) found concordance in directionality, their analyses suggest little temporal concordance. Although divergence and admixture between refugial populations are broadly concentrated in the late Pleistocene, the timing of divergence and admixture between refugia is to a large extent idiosyncratic across species. However, in order to to explore a plausible space of necessarily complex demographic scenarios which capture aspects of both the longitudinal colonisation history (divergence between refugia) and the more recent history of latitudinal range shifts (admixture between refugia), Bunnefeld et al. (9) had to make drastic simplifying assumptions about the second major axis of demographic history: population size change. Specifically, their analyses assumed a single fixed effective population size per refugium. This immediately raises the question of whether the lack of temporal concordance of species' histories found by Bunnefeld et al. (9) is a property of the broad spatial and deep temporal scale captured by their models, or whether it is a much more general property of the history of ecological communities which holds over a range of spatio-temporal scales. There are several reasons to expect temporal concordance to depend on spatial and temporal scales (47). For example, of colonisation and admixture events may be idiosyncratic simply because they are determined by long-distance dispersal events which both depend on a species' dispersal ability (Smith et al.) and are inherently random.

Here we use whole genome sequence (WGS) data to quantify and compare the histories of population size change within a single glacial refugium across seven chalcid parasitoid species in the oak gall wasp community previously studied by (9). We focus on the Iberian refugium, which for most species in the oak gallwasp parasitoid community represents the end-point of a longitudinal expansion history: Iberian populations have lower genetic diversity than more eastern refugia, show little evidence of population structure (52; 60; 44) (for an exception see Rokas et al. (51), and are least affected by post-colonisation gene flow from other refugia (62; 9). Our sampling targets males (five from Iberia, one from the Balkans in each species), whose haploid genome facilitates analysis (9; 23). WGS data allow for powerful demographic inference even for non-model organisms. However, given fragmented reference genomes and limited sample sizes available for these species, inference methods must be chosen carefully and, ideally, should use linkage as well as allele frequency information. In particular, inference based only on the site frequency spectrum (SFS) (e.g. 20) requires larger samples for accurate inference of recent population history.

We investigate the history of population size change in Iberia using two approaches that use the signal contained in genome-wide variation of a small sample of individuals in different ways (9; 38; 34). We use a parametric maximum-composite likelihood (MCL) method based on a blockwise summary of sequence variation (38) (hereafter termed the 'blockwise method') to fit a model of a single instantaneous step change

in N_e. Using analytic likelihood calculations to fit such fully specified but minimally complex histories utilises both frequency and linkage information and facilitates statistical comparison between species for the timing and magnitude of N_e change. We also applied a non-parametric method commonly used to visualize population size change, the Pairwise Sequentially Markovian Coalescent (PSMC) (34), which is based on the distribution of pairwise differences in minimal samples of two haploid genomes. PSMC generates a more resolved picture of N_e change through time, including a qualitative assessment of the time at which populations have diverged. As the two methods make opposing assumptions, we will not attempt any formal comparison between them but rather compare inferences qualitatively. Both methods use different data properties and sampling strategies and, as a consequence have contrasting limitations: while the blockwise method – by design – cannot detect gradual N_e changes or resolve population histories involving multiple changes, PSMC is known to smooth out very sudden changes. PSMC is based on fewer samples which contain less information (i.e. fewer coalescence events) about the recent N_e (34). The two methods therefore complement each other and together provide a comprehensive picture of population history.

We address the following questions: *(i)* To what extent are the direction and timing of changes in N_e concordant across members of the oak-gall parasitoid guild? Do species show evidence for simultaneous N_e change suggesting concordant responses to a shared underlying driver, or are their demographic histories largely idiosyncratic as shown by Bunnefeld et al. (9) for the timing of divergence and admixture between refugia? *(ii)* Do sudden changes in population size coincide with specific glacial or interglacial periods in the Pleistocene? *(iii)* Do the most drastic demographic changes occur after the colonisation of Iberia, or are they shared with other refugial populations, suggesting that genetic diversity in Iberia largely reflects the size of the ancestral source populations?

Materials and Methods

Samples and sequencing

We analysed whole genome Illumina paired end resequencing data for six (haploid) male individuals in each of seven species of chalcid parasitoids (spanning five families): *Megastigmus dorsalis* and *M. stigmatizans* (Megastigmidae), *Torymus auratus* (Torymidae), *Ormyrus nitidulus* and *O. pomaceus* (Ormyridae), *Eurytoma brunniventris* (Eurytomidae) and *Cecidostiba fungosa* (Pteromalidae) (Table S1). The *M. dorsalis* individuals correspond to cryptic species 1 for this complex, as defined by Nicholls et al. (44). For each species, we sampled five individuals from Iberia (the focal refugial population) and one from Hungary (the

Balkan refugium). Data for the Hungarian and two Iberian samples of each species were generated previously by Bunnefeld et al. (9). We generated analogous data for the remaining three Iberian individuals using the protocols described by Bunnefeld et al. (9). DNA was extracted from individual wasps using the Qiagen DNeasy kit. Individual Nextera genomic libraries were generated and sequenced on an Illumina HiSeq 2000 by the NERC Edinburgh Genomics facility, UK. Raw reads were deposited at the SRA (PRJEB20883). Mean coverage per haploid individual ranged from 3.5x to 18.5x. Raw reads were mapped back to reference genomes assembled by Bunnefeld et al. (9) using *BWA* (0.7.15-r1140) (33), duplicates were marked with *picard* (V2.9.0) MarkDuplicates (broadinstitute.github.io/picard/), variants were called using *Freebayes* (v1.1.0-3-g961e5f3) (https://github.com/ekg/freebayes) with a minimum base quality of 10 and a minimum mapping quality of 20 (see Bunnefeld et al. (9) for further details).

Inferring step changes in population size

We fitted a model of a single instantaneous step change in N_e using the framework for blockwise likelihood calculations developed by Lohse et al. (38). The model includes three parameters: the scaled mutation rate $\theta = 4N_0\mu\times\ l$ (where N_0 is the current N_e and l is block length); T, the time of N_e change measured in $2N_e$ generations; and $\lambda = N_0/N_1$, the relative magnitude of the N_e change, (where N_1 denotes the N_e prior to the step change).

Following Bunnefeld et al. (8), we summarized sequence variation in short blocks of a fixed length l by the (folded) blockwise site frequency spectrum (bSFS) using the script *block_cutter_vcf.py* (https://github.com/KLohse/BunnefeldEtAL_2018/block_cutter_vcf.py). Given our sampling scheme of $n = 5$ haploid males, the bSFS consists of counts of two types of variants: those for which the minor allele occurs once or twice in the sample. The probability of observing a particular set of mutations in a block can be computed analytically as a higher-order derivative of the generating function of genealogies (38). The product of probabilities of bSFS configurations across blocks can be interpreted as the composite likelihood (CL) of the model. We maximised $lnCL$ in *Mathematica* (70) using the function *NMaximise* (Supplementary File 1).

To generate blockwise data for each species, we applied the same quality filters used for calling SNPs to all sites, i.e. we identified regions of the genome with a base quality >10 and mapping quality >20 in each individual from bam files by the CallableLoci walker of *GATK* (v3.4) (64). Only regions meeting these criteria in all five Iberian individuals were included in further analyses. Custom scripts were used to partition the data into blocks of a fixed length l of callable sites. l was chosen to be inversely proportional to the pairwise genetic diversity of each species (Table 2), such that blocks, each capturing a random configuration

of closely linked variants had an average two pairwise differences between samples. This ensures that the information content per block as well as any effect of intra-block recombination is consistent across species. Blocks with a physical span (including non-callable sites) of $> 2l$, contigs with length $< 2l$, and blocks with more than five "None" (uncalled) sites were removed.

We assessed support for a step change in N_e relative to the (nested) null model of constant N_e by generating parametric bootstraps with the coalescent simulator *msprime* (30). For each species, 100 replicate data sets were simulated under the null model assuming estimates of recombination inferred by Bunnefeld et al. (9) (Table S3). Each dataset had the same total length as the real data (after filtering) and was partitioned into 5,000 windows of sequences (for computational efficiency). Both a null model of constant N_e and a step change model were fitted to each replicate, and the 95% quantile of the difference in support between models $lnCL$s was compared to that of the real data. Confidence intervals (CIs) of parameter estimates were obtained via an analogous parametric bootstrapping procedure: we simulated 100 datasets with recombination under the inferred step change model and fitted that model to each simulation replicate. CIs were obtained as 2.5% and 97.5% quantiles of the distribution of parameter estimates, and were centred around the point estimates of parameters obtained from the real data.

Reconstructing ancestral population size with PSMC

The Pairwise Sequentially Markovian Coalescent (PSMC) (34) was used to infer a history of population size change in each species. PSMC is a non-parametric method that reconstructs a trajectory of past N_e from the density of pairwise differences along the genome via a hidden Markov model in which the hidden states are pairwise coalescence times, the distribution of which is used to estimate N_e in discrete time intervals. In each species, the two Iberian individuals with the greatest average read depth were used as the focal pair. Pileup files were generated using *samtools mpileup (version 0.1.19)* (35) and a consensus sequence (fastq file) per individual was generated using the bcftools utility vcf2fq. Regions covered in both individuals were combined into fastq files using *seqtk mergefa* (https://github.com/lh3/seqtk) and converted into PSMC input files. PSMC, by default, discretizes pairwise alignments into blocks of 100bp which are encoded as variant if they contain at least one variant. While this makes analyses of large genomes with low diversity (e.g. humans) computationally efficient, this discretisation is too coarse when considering more diverse genomes where the chance of several pairwise differences occurring in the same 100 bp block is non-negligible (which biases N_e estimates downwards). We investigated the effect of varying block length (100, 50, 25 and 1bp) on N_e inference for the most diverse (*E. brunniventris*, $\pi = 0.0071$) and the least diverse (*M. stigmatizans*

$\pi = 0.00067$) species in our set. As expected, population trajectories showed higher N_e and were pushed back in time with smaller block lengths (Figure S1). We chose a block length of 25bp for all analyses which minimizes these biases without excessive computational cost.

We inferred 30 free interval parameters across 64 time intervals (with the option -p "28*2+3+5"). The maximum coalescence time (-t) was set to 5, the initial value of θ/ρ (-r) to 1. 100 bootstraps were performed for each run. Times of peak N_e and values of N_e in each time interval were considered to be different between species if there was no overlap in bootstrap replicates. To be able to compare the magnitude of inferred N_e change between PSMC and blockwise analyses, we normalised the maximum N_e inferred by each method by the long-term average N_e estimated simply from π (42) (Table 2) as $\hat{N_{e,\pi}} = \pi/(4\mu)$ and computed the following measure of N_e change: $Max[N_e]/\hat{N_{e,\pi}}$. Unlike the size of the step change (λ), this measures the maximum N_e relative to the average over the entire history of a sample and is therefore expected to be smaller than λ.

Calibrating the timing of events

Time estimates were converted into years assuming a mutation rate of 3.46×10^{-9} mutations per base per generation estimated for *Drosophila melanogaster* (29). We assumed two generations per year for all species with the exception of *M. stigmatizans* which has a single generation per year (59). While this calibration allows comparisons with the estimates obtained by Bunnefeld et al. (9) (calibrated in the same way), these absolute times are likely underestimates and should be treated with caution (given that we use a spontaneous mutation rate estimate and not all *de novo* mutations are selectively neutral). We stress, however, that comparing the relative timing of demographic events across this set of parasitoids only relies on the assumption of the same per generation mutation rate across species rather than any absolute calibration.

Cross-population PSMC analyses

To test whether population size changes in each species occurred before or after the divergence between the Iberian and Balkan refuge populations, we compared the PSMC trajectories of Iberian pairs and cross-population pairs (one Iberian and one Hungarian individual). Any divergence between Iberian and the Balkan refuge populations should be visible as a separation between the within-population (Iberian pair) and the cross-population (Iberia-Balkan pair) PSMC trajectories. Specifically, in the absence of significant post-divergence gene flow we expect N_e estimates for the cross-population pairs to increase from the time of the population split due to the accumulation of genetic differences between the populations. Thus population size

changes that occurred in an ancestral population (potentially outside Iberia) should predate the divergence of within and cross-population trajectories. In contrast, we would expect demographic events unique to the Iberian population to happen after divergence of the within- and cross-population PSMC trajectories. We also compared our PSMC divergence time estimates to those made by Bunnefeld et al. (9) under explicit models of divergence and admixture.

Potential population structure in Iberia

Population structure within any assumed panmictic population (here, Iberia) can confound inferences of past demography (18; 8). In particular, N_e estimates may be inflated due to divergence between demes (18). Likewise, when samples are taken from the same deme, the (structured) coalescent generates a mixture of very recent within-deme ancestry and older ancestry resulting from migration between demes (66), which can mimic the signatures of a bottleneck (8). To test for population structure within Iberia, we repeated PSMC analyses on every pairwise combination of our five individuals. In a structured population, and given that the sampling locations were widely spaced across Iberia (Table S1), N_e trajectories are expected to differ between pairs of haploid males sampled from the same *versus* different sub-populations (analogous to the within- and between-population analyses involving Iberian and Hungarian samples).

Sensitivity analyses

The assumption of no recombination within blocks (which is required to make the composite likelihood estimation tractable) potentially leads to biases in parameter estimates. Specifically, recombination may lead to a downward bias of N_e estimates (67; 8). We used simulations in *msprime* (30) to quantify the effect of recombination on parameter estimates (Table S2). One million unlinked blocks of 586bp (corresponding to the block length used for *O. nitidulus*) were simulated under a step change model with different recombination rates and step sizes.

It is well known that both selective sweeps (56) and background selection (11) affect variation at neutral sites in the genome which, in turn, can bias demographic inference (16; 54). To explore the effect of selection on the blockwise analyses, we fitted step change models separately to blockwise data generated from genic and intergenic regions of the *O. nitidulus* genome. Genes were predicted *ab initio* with *Augustus* (58). *Nasonia vitripennis*, a chalcid parasitoid (family Pteromalidae), was used as a training set. If selection has a strong effect on demographic inference, estimates of θ are expected to be much lower for genic compared to intergenic regions, as most selection tends to reduce diversity both at selective targets and linked regions

of the genome (56). Similarly, we would expect estimates for the time of the step change, T, to be biased towards the present in genic compared to intergenic regions.

Results

After filtering, the blockwise datasets ranged in total length from 54 to 151 Mb (Table S3). The pairwise alignments used as input for PSMC spanned a total length of 161 to 379 Mb (Table S3). Despite this difference in overall length, which is mainly a due to missing data and the difference in sample size (two *versus* five individuals), estimates of average pairwise diversity, as measured by π (42), agreed broadly between the two datasets and were slightly lower for the blockwise data (Table 1) compared to the pairwise alignments (Table 2). Across species, π estimates spanned an order of magnitude, from 0.00067 in *M. stigmatizans* to 0.0071 in *E. brunniventris*.

Large changes in N_e detected in four species

Taking the results of the blockwise and PSMC analyses across all seven parasitoid species together, four species (*M. stigmatizans, M. dorsalis, O. nitidulus* and *T. auratus*) show evidence for large (at least a factor of three) changes in population size during the Quaternary period (Figure 1). In these species, an instantaneous step change in N_e fits the blockwise data significantly better than a null model of a constant N_e. We infer a decrease in N_e towards the present ($\lambda < 1$) in three species (*M. stigmatizans, M. dorsalis* and *O. nitidulus*) and an increase in one species (*T. auratus*) ($\lambda > 1$) (Figure 1 and Table 1). In all four species, the change in N_e in the PSMC trajectory (Figure 1) agrees both in direction and coarse timescale with the inference under the single step-change model. However, the N_e changes visible in the PSMC trajectory for these species are not equally abrupt. For example, *T. auratus* shows a gradual increase of N_e over a period of more than 200 ky, while the decreases in the PSMC trajectories of *M. dorsalis* and *M. stigmatizans* are comparatively sudden. PSMC trajectories and inferences based on blockwise analyses are also broadly similar for *O. pomaceus* and *C. fungosa*: a step change in N_e is supported in neither species, and PSMC suggests comparatively small population size changes for both (Tables 1 and 2).

However, while we have resisted the temptation to attempt any formal comparison between PSMC trajectories and inferences under the single step change model which would necessary be *post hoc* and potentially misleading (given the opposing assumptions of these methods, see Discussion), inferences under the two methods disagrees qualitatively in at least two obvious ways:

First, with the exception of *M. stigmatizans*, the magnitude of N_e change inferred under the step-change model is greater than the relative magnitude of peak N_e in the PSMC trajectories (Figure 1, Tables 1 and 2). Second, in one species, *E. brunniventris*, blockwise and PSMC analyses are hard to reconcile: although we found no significant support for a step change for this species, i.e. we cannot reject a null model of a single fixed N_e. Yet, the PMSC trajectory indicates a substantial (but gradual) increase in N_e (Table 2). Additional analyses for this species (see Discussion) suggest that demographic inferences for *E. brunniventris* may be affected by genetic structure and/or the low contiguity of its reference genome.

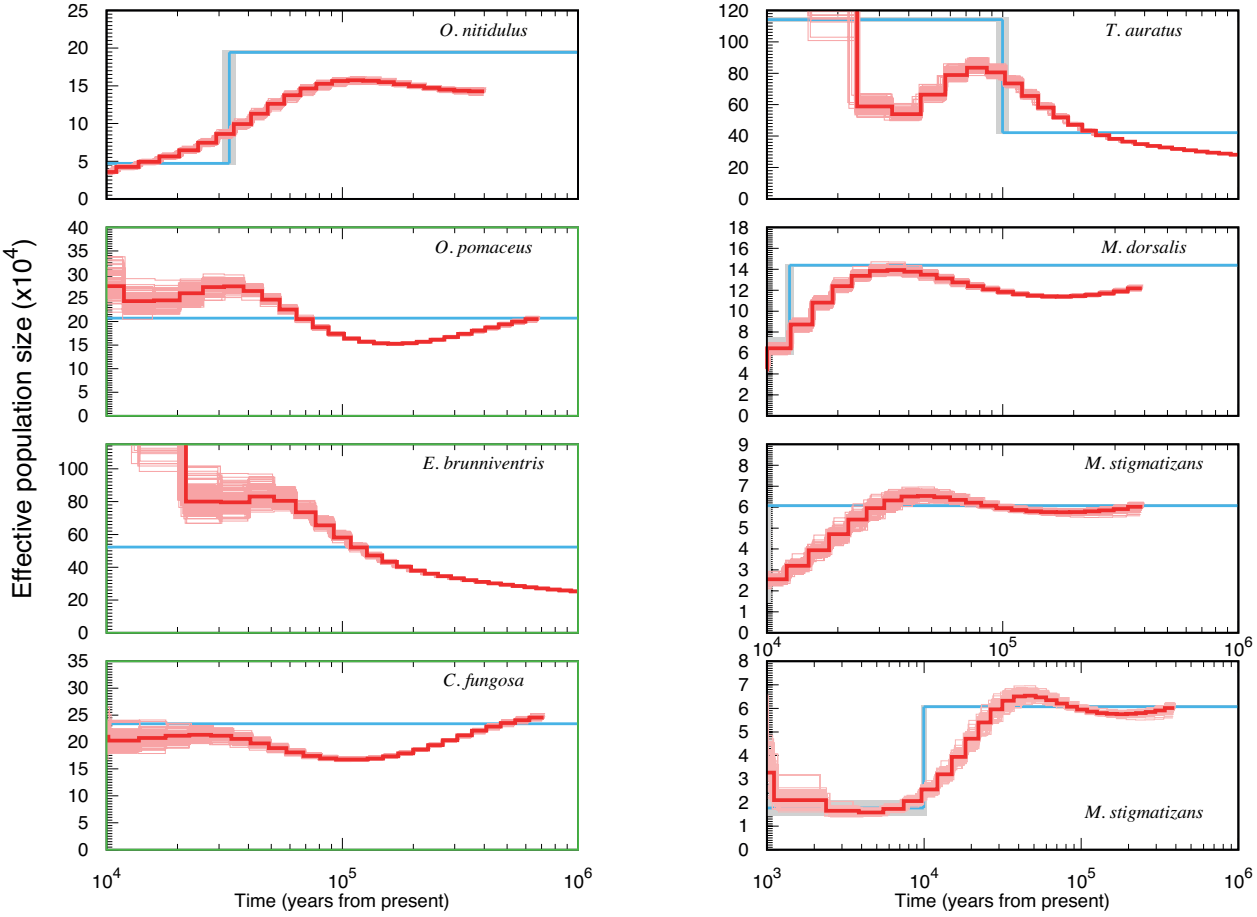

Figure 1: PSMC and maximum composite likelihood estimates (MCLE) of N_e for Iberian populations of seven species of chalcid parasitoid wasps. PSMC estimates and bootstrap replicates are shown in dark red and pale red, respectively. Population sizes estimated using the composite likelihood step change model are shown in blue with 95% CIs in grey. The three species with green plot frames are those for which a step change model is not supported. Results for *M. stigmatizans* are also plotted on an alternative timescale to reveal recent N_e change (bottom right).

Table 1: Maximum composite likelihood estimates (MCLE) of demographic parameters for Iberian populations of seven species of chalcid parasitoid wasps under a model of a single step change. Estimates for the time of N_e change (T) are given in thousands of years ago (kya). 95% CIs are shown in brackets. The maximum N_e is scaled relative to π as $Max[N_e]/N_{e,\pi}$.

Species	π	**Current** $N_e \times 10^3$	**Ancestral** $N_e \times 10^3$	T **(kya)**	**Relative** $Max[N_e]$
T. auratus	0.00509	1,142 (1,126-1,157)	422 (418-425)	100 (94-106)	2.14
M. stigmatizans	0.00054	18 (14-21)	61 (60-61)	10 (9.5-10.4)	1.55
M. dorsalis	0.00142	67 (59-75)	144 (143-145)	12.5 (12.0-13.0)	1.40
O. nitidulus	0.00126	47 (45-49)	194 (192-197)	33 (31-35)	2.13
O. pomaceus	0.00230	207 (207-208)	n/a	n/a	n/a
E. brunniventris	0.00569	523 (521-525)	n/a	n/a	n/a
C. fungosa	0.00258	234 (233-235)	n/a	n/a	n/a

Table 2: Summaries of PSMC trajectories for Iberian populations of seven species of chalcid parasitoid wasps. Times are given in thousands of years ago (kya). 95 % CIs of peak N_e times are shown in brackets. The maximum N_e is scaled relative to *pi* as $Max[N_e]/N_{e,\pi}$.

Species	π	**Peak** $N_e \times 10^3$	**Peak** N_e **time (kya)**	**Split time (kya)**	**Relative** $Max[N_e]$
T. auratus	0.0064	835	78 (74-82)	n/a	1.81
M. stigmatizans	0.00067	65	47 (42-52)	37	1.34
M. dorsalis	0.0018	139	35 (31-39)	128	1.07
O. nitidulus	0.0016	157	114 (104-124)	132	1.36
O. pomaceus	0.0028	275	35 (30-40)	681	1.36
E. brunniventris	0.0071	831	46 (36-56)	n/a	1.62
C. fungosa	0.0032	213	25 (12-38)	267	0.92

No support for temporal concordance of population size change

The four species with support for a step change in N_e (*M. stigmatizans, M. dorsalis, O. nitidulus* and *T. auratus*) show no overlap in the estimated times of N_e change (Table 1). Using an insect spontaneous mutation rate (29) to calibrate T estimates (see Methods for caveats), Iberian populations of *M. stigmatizans* and *M. dorsalis* most likely decreased in size at the start of the current interglacial (10 and 12.5 kya respectively). In contrast, the decrease in N_e inferred for *O. nitidulus* most likely dates to the last glacial period (33 kya) and the increase in N_e in *T. auratus* at 100 kya dates to just after the end of the (Eemian) interglacial (Table 1). Formalising this comparison, we conclude that a maximally complex model that assumes a unique time of N_e change for each of the four species fits significantly better than any scenario involving concordant/clustered times of N_e change.

Comparing times of N_e change inferred via PSMC across species is inherently problematic (see Discussion). However, comparing the time of maximum N_e across species by computing the overlap in peak N_e intervals across bootstrap replicates, we find that the four taxa *M. stigmatizans, M. dorsalis, O. nitidulus* and *T. auratus* which show support for a single step change at unique times also have non-overlapping peak N_e times (Table 1). Interestingly, the three species with no support for a step change (*O. pomaceus, C. fungosa* and *E. brunniventris*) as well *M. dorsalis* show highly similar (overlapping CI) times of peak N_e (Figure 2 and Table 2).

Changes in N_e occur after the divergence of Iberian populations

In five species the PSMC trajectories of within-population (Iberia) pairs diverge clearly from the cross-population (Iberia *versus* Hungarian) trajectories. In contrast, little divergence between within and cross-population PSMC trajectories is visible for *E. brunniventris* and none for *T. auratus* (Figure 3). In all three species for which the blockwise analyses support a decline in population size, the inferred time of N_e change is more recent than the divergence of within- and cross-population PSMC trajectories (Figure 3 and Table 2) and so must have occurred after Iberian and Balkan populations split. For *O. pomaceus*, *C. fungosa* and *M. stigmatizans* the split times between Iberian and the Balkan populations inferred here *post hoc* by comparing PSMCs trajectories are broadly compatible with the divergence estimates obtained by Bunnefeld et al. (9) under explicit models of population divergence (Figure 3). In contrast, for both *M. dorsalis* and *O. nitidulus* the divergence of within and between refuge PSMC trajectories substantially predate the split times inferred by Bunnefeld et al. (9). In both cases, cross-population PSMC trajectories decrease after divergence between the Iberian and Hungarian populations, suggesting that these populations have been connected by a period of

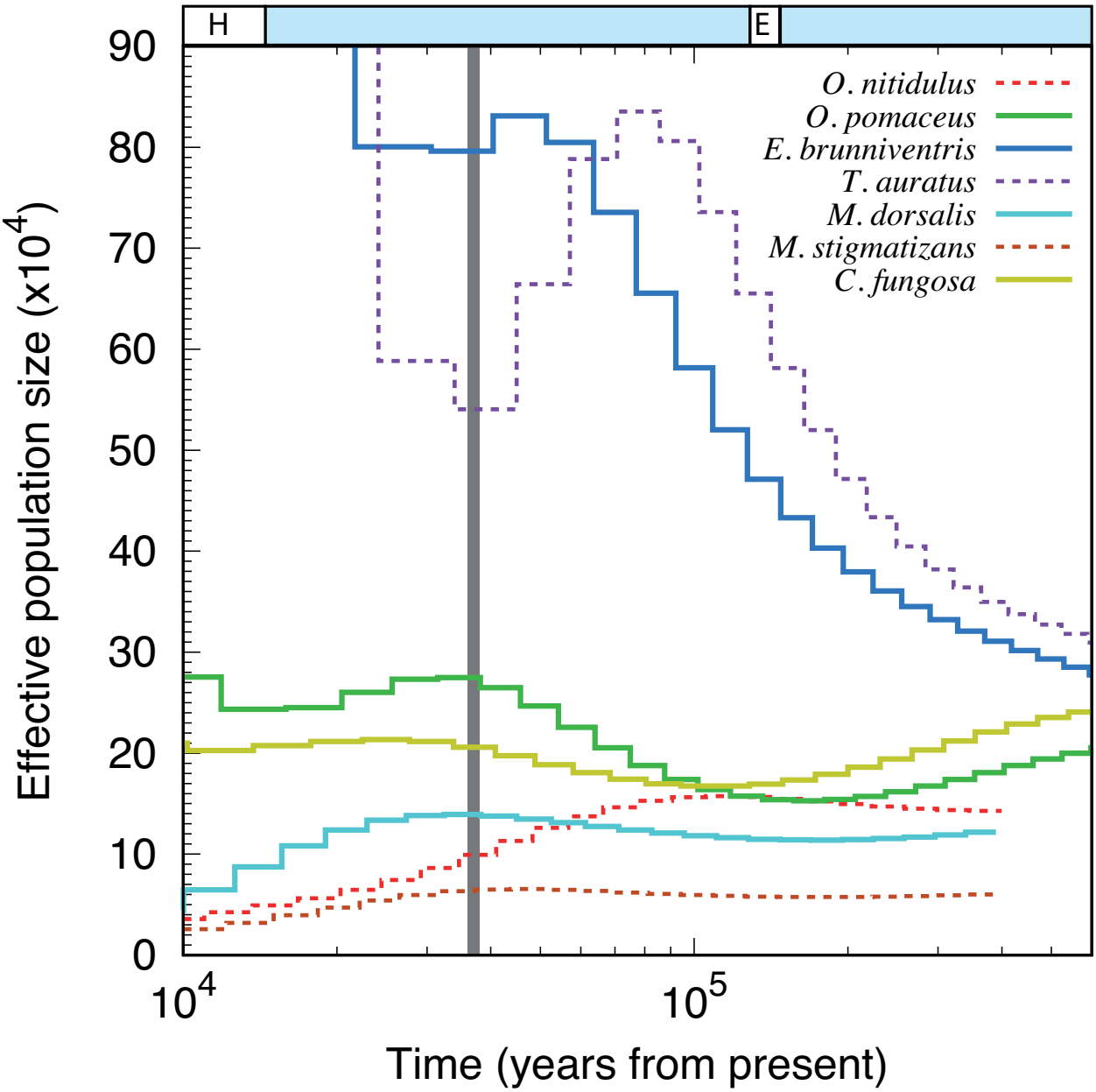

Figure 2: N_e trajectories inferred by PSMC for Iberian populations of seven species of parasitoids. The vertical grey bar indicates the overlap in the timing of peak N_e across 95 % CIs computed from bootstrap replicates across four species (solid lines) (*M. dorsalis, O. pomaceus, C. fungosa* and *E. brunniventris*). The remaining three species (dashed lines) have unique peak N_e times.The time bar along the top of the figure shows (from left to right) the Holocene (H, 11.7kya to present), the last glacial, the Eemian interglacial (E, 115-130kya) and the penultimate interglacial.

gene flow immediately following divergence which may not be detectable given the admixture pulse scenarios fitted by Bunnefeld et al. (9).

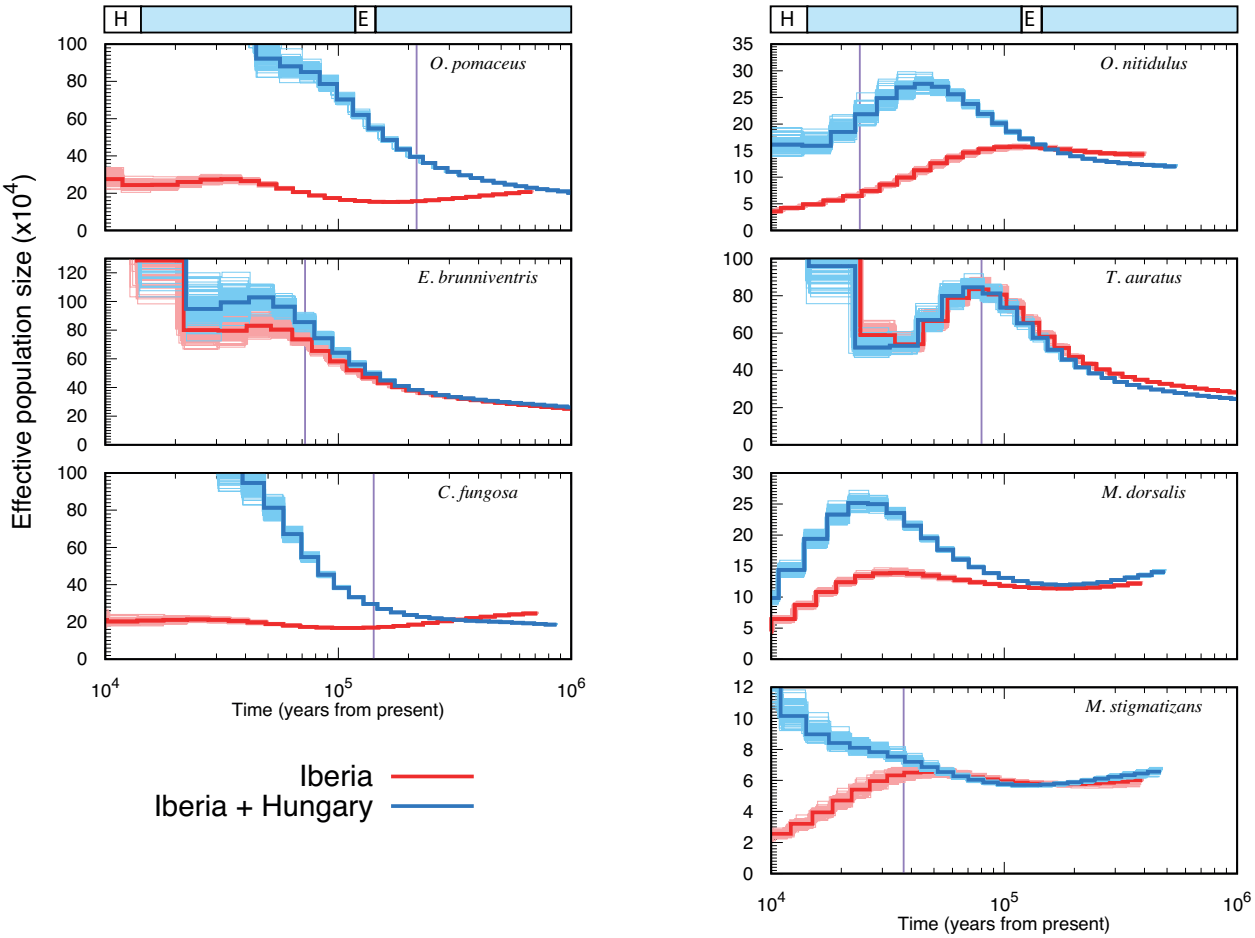

Figure 3: PSMC N_e trajectories for Iberian (red) and cross-population (Iberian vs Balkans) pairs (blue) of seven species of parasitoids. Population splits can be inferred as the time at which the trajectories of within-population and cross-population pairs diverge. Vertical bars indicate the split times estimated by Bunnefeld et al. (9) using a MCL method based on the blockwise data. The split time estimated by Bunnefeld et al. (9) for *M. dorsalis* is too recent (8 kya) to be visible in this figure. The time bar along the top of the figure shows (from left to right) the Holocene (H, 11.7kya to present), the last glacial, the Eemian interglacial (E, 115-130kya) and the penultimate interglacial.

No evidence for structure within Iberia

We find little variation in PSMC trajectories between different Iberian pairs in almost all species (Figure S2), suggesting that our demographic inferences are unlikely to be influenced by population structure within Iberia. For all species except *E. brunniventris*, the differences in PSMC trajectories between different Iberian sample pairs are similar to the differences across bootstrap replicates (Figuresw 1 S2), and so most likely

reflect coverage variation between individuals. *E. brunniventris* is the only species that showed clear variation in PSMC trajectories between Iberian pairs. While our additional analyses for *E. brunniventris* suggest other potential reasons for this finding (see Discussion), we cannot rule out that this variation is in part driven by population structure.

Sensitivity analyses

Both demographic inference methods used here assume selective neutrality but make different simplifying assumptions about recombination: while PSMC approximates recombination as a Markov process along the genome, the blockwise composite likelihood framework assumes no recombination within blocks. To check the extent to which recombination and selection may bias parameter estimates, we fitted histories of a step change to data simulated with recombination. Our exploration of simulated data shows that both N_e and λ are underestimated with increasing recombination rate whereas the time of step change (T) is biased downwards when N_e declines towards the present ($\lambda < 1$) and upwards when N_e increases ($\lambda > 1$) (Table S2). These biases are an expected consequence of the shuffling of genealogical histories within a block in the presence of recombination, which reduces the variance in bSFS configurations. Given a recombination rate of $r = 3 \times 10^{-9}$ estimated for the parasitoids, our simulation check suggests that while T, the time of the step change may be underestimated by up to a factor of two, the ability to accurately estimate λ, the magnitude of the step change is little affected.

To investigate the potential effect of selective constraint on the block based inference we fitted a history of a single step change separately to genic and intergenic regions. Parameter estimates based on genic data for *O. nitidulus* were similar to the full data set (Table S2). While N_e is slightly lower and T is slightly greater for genic regions, as would be expected as a result of selective constraints, the timing and relative magnitude of demographic change was little affected by partitioning the data by annotation.

Discussion

We analysed genome-wide sequence variation using two contrasting inference approaches to test if and how demographic histories vary within a guild of insect parasitoids in a single Pleistocene refugium. We find evidence for drastic declines in population size in three out of seven species (*M. stigmatizans, M. dorsalis, O. nitidulus*), and a large increase in population size one species (*T. auratus*). However, contrary to a simple scenario of guild-wide temporal concordance in responses to Pleistocene climatic events, we find that

population size changes of species in this guild differ markedly both in direction and timescale. In fact, our analyses assuming a single step change in N_e reveal significant support for maximal temporal discordance, i.e. each of the four species in this parasitoid guild that show evidence for a sudden change in N_e has a unique time (Table 1).

Thus our main result of temporally discordant N_e change within Iberia mirrors the finding of temporal discordance in Bunnefeld et al. (9) in the timing of divergence and admixture for this guild on a continental scale. One could argue that the signal of temporal discordance may simply be an artefact of applying an oversimple step-change model, which is unlikely to capture the subtleties of real population size change. However, the fact that we also find evidence for temporal discordance when visualising N_e change using PSMC, which makes minimal simplifying assumptions about the shape of past demographic change, suggests a genuine lack of signal for temporal concordance in this parasitoid guild across a range of spatio-temporal scales. This general finding mirrors results of other comparative studies on sets of co-distributed taxa in Europe (15) and North America (14; 10).

It is interesting that the only potential signal of temporal concordance we find is for four species that show the smallest change in past population sizes and which overlap in the time of peak N_e. While this apparent congruence may be due to a shared background demography, the signatures of which are masked in species with more drastic changes in N_e, we cannot rule out alternative explanations. In particular, the fact that PSMC assumes selective neutrality is problematic given that insect genomes are more compact that mammalian genomes (36) and so more susceptible to the effects of linked selection. Schrider et al. (54) have shown that selective sweeps can generate troughs in PSMC trajectories while background selection has been shown to lead to erroneous inference of population growth (16). We therefore cannot rule out the possibility that congruent peaks in N_e are an artefact of selective effects which, assuming similar genome composition, mutation, and recombination rates, may distort PSMC inferences in similar ways. However, the fact that we have reconstructed strikingly different PSMC trajectories, most of which differ markedly from the selection-induced PSMC trajectories of Schrider et al. (54) (in that they show large declines rather than increases in N_e toward the present), suggests that it is unlikely that linked selection is the main driver of the inferred N_e changes. For the blockwise analyses we find little difference in parameter estimates between genic and intergenic regions of *O. nitidulus* (Table S2), which again argues against a major effect of selection on our inferences. Furthermore, one would expect genomes with a shorter map length (physical length $\times$ recombination rate) to be disproportionately affected by linked selection (56; 40). However, if anything, we observe the opposite pattern: the two species with shortest map lengths (*O. nitidulus* and *C. fungosa*)

show less pronounced N_e change than the two species with the longest map length (*M. stigmatizans* and *M. dorsalis*).

Reconciling step change and PSMC analyses

PSMC and blockwise analyses exploit different aspects of the data and differ drastically in sampling schemes (contiguous pairwise alignments vs short blocks sampled across five individuals) and underlying assumptions: while the blockwise composite likelihood framework fits a single instantaneous step change in N_e and infers the timing of this event, PSMC does not estimate a time parameter *per se* but rather imposes an arbitrary discretization of time and reconstructs population size change as a continuous trajectory. It is reassuring that despite these fundamental differences, both methods yield broadly congruent conclusions: the four species for which the blockwise analyses diagnose an abrupt change in N_e also show PSMC trajectories with large N_e changes in the same direction and at similar times. The greater magnitude of N_e change under the step change history compared to the PSMC analyses may be a consequence of the fact that larger samples analysed in the blockwise framework contain more information about recent demography than a pair of lineages.

In general, one may view the fact that PSMC is essentially assumption-free as an advantage over model based inference, because it enables a straightforward visualisation of past N_e change. Similarly, comparing PSMC trajectories between pairs of individuals and populations allows qualitative assessment of likely periods of divergence and admixture (Figure 3). However, the flip-side of this flexibility is that PSMC provides no obvious route for quantitatively testing (necessarily) simple demographic hypotheses across species. Furthermore, cross-species comparisons of PSMC trajectories are problematic even when they are focused on a single clearly defined summary such as the interval of peak N_e (as we have done here) because the discretisation of time PSMC imposes depends on the time scale of coalescence and so differs between species.

Changes in population size coincide with late Pleistocene climatic transitions

While we emphasize that absolute time estimates need to be interpreted with caution, our estimates of the timing of drastic N_e changes coincide broadly with climatic events in the Quaternary: the start of the Holocene around 11 kya, and the end of the Eemian interglacial around 106 kya (Figure 3). Previous studies on the parasitoid oak gallwasp community based on the same calibration have inferred an increase in gene flow between refugia during the same time periods (9; 39; 37). For example, the cluster of peak N_e times coincides with a large community-wide peak in the frequency of admixture between refugia inferred by Bunnefeld et al. (9). Similarly, the increase in N_e for *T. auratus* at the end of the Eemian interglacial period coincides with the

divergence of the Iberian population of this species inferred previously (9; 59). It seems plausible that both events are associated with the geographic expansion of suitable oak habitat across refugial barriers during these times (7; 48), which may have triggered range expansions in both host gallwasps and their associated parasitoids.

Population structure within Iberia and gene flow from Eastern refugia

Population structure within southern European refugia has previously been demonstrated for some species, and it has been suggested that given its complex topography Iberia should be considered a mosaic of multiple micro-refugia rather than a single entity (17; 23). However, our PSMC results suggest a complete lack of population structure in six out of seven species in the parasitoid guild (Figure S2) and imply high gene flow within Iberia. This is perhaps unsurprising given that gallwasp-associated parasitoid wasps (and other chalcids) are able to disperse long distances even across patchy habitats and host distributions (22; 13).

Our estimates of population split times based on comparisons of within- and cross-population PSMC trajectories agree broadly with those of Bunnefeld et al. (9) for most species. *M. dorsalis* and *O. nitidulus*, the two species that show the least agreement with past estimates, both show decreases in cross-population N_e after divergence that are compatible with ongoing gene flow between refugia. The model space considered by Bunnefeld et al. (9) was limited to histories involving a single discrete burst of instantaneous admixture between refugial populations, with limited potential to detect periods of continuous post divergence gene flow.

E. brunniventris is an outlier

E. brunniventris is an outlier in our results in several ways: it is the species with the highest genetic diversity, shows signals of population structure within Iberia, and is the only species for which our two inference approaches disagree. While the blockwise analysis gives no support for a change in N_e, the PSMC trajectory shows a steady increase. To explore the ability of the blockwise analyses to detect gradual changes in population size, we simulated 100 replicate data sets (assuming the same size and block length as the real data) under the gradual change in N_e inferred via PSMC for *E. brunniventris*. We find that in each case, a history of a single step change fits the data significantly better (using a parametric bootstrap analogous to taght performed on the real data, see Methods) than a null model of constant N_e, indicating that the blockwise analysis is indeed sensitive to gradual increases in population size. A possible explanation for the discrepancy between the PSMC and blockwise inferences for *E. brunniventris* is that its genome assembly,

the least contiguous among our set of taxa (Table S1), is too fragmented for reliable PSMC inference. Interestingly, both a history of constant N_e and a step change model give a poor fit to the observed frequency of bSFS configurations in *E. brunniventris*. In particular, *E. brunniventris* shows an excess of both monomorphic blocks and blocks with a large number of variants (Figure S3), suggesting that its history is not well approximated by any model that assumes a single panmictic population. The lack of divergence of within- and between-population PSMC trajectories for *E. brunniventris* would be compatible with substantial gene flow between the Iberian and Hungarian populations (Figure 3). Alternatively *E. brunniventris* – an extreme generalist attacking a wide range of oak gallwasp hosts (2) – may harbour genetic structure as a result of recent divergence into cryptic host races (45) However, in the absence of a better reference genome and larger sample sizes it remains unclear to what extent the disagreement between PSMC and blockwise analyses for *E. brunniventris* is indicative of a more complex history.

Outlook

A general question for geographically widespread communities is the extent to which component species continue to interact during the assembly process (28; 1; 50). Where communities are characterised by strong dependencies between species, such as specific trophic or symbiotic interactions, we might expect co-dispersal and coupled population dynamics to result in similar demographic histories (e.g. 19); this scenario is compatible with ongoing selective effects of species on each other, and potential coevolution (41; 21).

In contrast, we might expect much lower demographic concordance for members of communities characterised by weaker and less specific species interactions and only diffuse coevolution (21). This is the pattern emerging for the parasitoid assemblages attacking oak gallwasps. Though comprising a consistent set of interacting taxa spanning thousands of kilometres of longitude, the component species show highly diverse histories of range expansion (9) and changes in population size. This finding is consistent with the ability of most of the parasitoid species to attack multiple gallwasp hosts (2), weakening both direct interactions between the trophic levels and competitive interactions between parasitoid species. While there is strong evidence that host gallwasp traits structure associated assemblages of parasitoid enemies (4), and of parasitoid specialisations for exploitation of particular hosts (69), there is little evidence for specific coevolution. The population histories of very few other multitrophic communities have been explored, and the extent to which the demographic diversity within the gallwasp system is typical of parasitoid-host and other biological systems remains unknown. Work on the arthropod communities associated with the pitcher-plant *Sarracenia alata* (53) also shows variation in component species histories; further, this study suggests that more ecologically

dependent associates show closer demographic and phylogeographic concordance with the host plant than less ecologically dependent species. An obvious question is whether any of the variation in patterns of N_e change in our sampled parasitoid species can be attributed to variation in ecological traits (47). Intriguingly, the four parasitoid species with support for a step change (in either direction) have a narrower host range (2) and a lower ancestral N_e than those for which a null model of constant N_e could not be rejected (Table S1). Although the number of species studied here is clearly insufficient for any statistical test of an association between host range and demographic history, these trends are compatible with the idea that ecologically specialist species (whose biology is critically dependent on interactions with a small number of other taxa) experience greater and/or more frequent changes in N_e than generalists (whose demography is less tightly coupled to abundance of any specific interaction) (49; 46). Larger samples of species, incorporating wide diversity in host number and other relevant traits (such as dispersal ability) are required to assess the extent to which life history traits and demographic histories are correlated. Given that the genomes of parasitoid wasp can be sampled in a haploid state (by targeting males), it will be fascinating to test how much more signal about the demographic past of ecological communities can be extracted using a new generation of inference approaches that reconstruct the sequence of correlated genealogies directly from the data (31; 57).

Acknowledgements

We thank Lynsey Bunnefeld for help in the molecular lab and useful discussions and José Luis Nieves-Aldrey and Juli Pujade-villar for contributing samples and Sam Ebdon for comments on the manuscript. This work was supported by a Natural Environment Research Council to GNS and KL (NE/J010499/1). WW was supported by an E3 doctoral training studentship from the Natural Environment Research Council (NERC) UK, KL is supported by a NERC fellowship (NE/L011522/1) and an ERC starting grant (ModelGenomLand).

References

[1] Agosta, S. J. and Klemens, J. A. (2008). Ecological fitting by phenotypically flexible genotypes: implications for species associations, community assembly and evolution. *Ecology Letters*, 11(11):1123–1134.

[2] Askew, R. R., Melika, G., Pujade-Villar, J., Schönrogge, K., Stone, G. N., and Nieves-Aldrey, J. L. (2013). Catalogue of parasitoids and inquilines in cynipid oak galls in the West Palaearctic. *Zootaxa*, 3643(1):1–133.

[3] Avise, J. C., Arnold, J., Ball, R. M., Bermingham, E., Lamb, T., Neigel, J. E., Reeb, C. A., and Saunders, N. C. (1987). Intraspecific phylogeography: The mitochondrial dna bridge between population genetics and systematics. *Annual Review of Ecology and Systematics*, 18(1):489–522.

[4] Bailey, R., Schönrogge, K., Cook, J. M., Melika, G., Csóka, G., Thuróczy, C., and Stone, G. N. (2009). Host niches and defensive extended phenotypes structure parasitoid wasp communities. *PLOS Biology*, 7(8):1–12.

[5] Beichman, A. C., Huerta-Sanchez, E., and Lohmueller, K. E. (2018). Using genomic data to infer historic population dynamics of nonmodel organisms. *Annual Review of Ecology, Evolution, and Systematics*, 49(1):433–456.

[6] Bermingham, E. and Avise, J. C. (1986). Molecular zoogeography of freshwater fishes in the southeastern united states. *Genetics*, 113(4):939–965.

[7] Brewer, S., Cheddadi, R., de Beaulieu, J., and Reille, M. (2002). The spread of deciduous Quercus throughout Europe since the last glacial period. *Forest Ecology and Management*, 156(1-3):27–48.

[8] Bunnefeld, L., Frantz, L. A. F., and Lohse, K. (2015). Inferring bottlenecks from genome-wide samples of short sequence blocks. *Genetics*, 201(3):1157–1169.

[9] Bunnefeld, L., Hearn, J., Stone, G. N., and Lohse, K. (2018). Whole-genome data reveal the complex history of a diverse ecological community. *Proceedings of the National Academy of Sciences of the United States of America*, 115(28):E6507–E6515.

[10] Burbrink, F. T., Chan, Y. L., Myers, E. A., Ruane, S., Smith, B. T., and Hickerson, M. J. (2016). Asynchronous demographic responses to pleistocene climate change in eastern nearctic vertebrates. *Ecology Letters*, 19(12):1457–1467.

[11] Charlesworth, B., Morgan, M. T., and Charlesworth, D. (1993). The effect of deleterious mutations on neutral molecular variation. *Genetics*, 134(4):1289–1303.

[12] Comps, B., Gömöry, D., Letouzey, J., Thiébaut, B., and Petit, R. J. (2001). Diverging trends between heterozygosity and allelic richness during postglacial colonization in the european beech. *Genetics*, 157(1):389–397.

[13] Compton, S. G., Ellwood, M. D. F., Davis, A. J., and Welch, K. (2000). The Flight Heights of Chalcid Wasps (Hymenoptera, Chalcidoidea) in a Lowland Bornean Rain Forest: Fig Wasps are the High Fliers. *Biotropica*, 32(3):515–522.

[14] DASMAHAPATRA, K. K., LAMAS, G., SIMPSON, F., and MALLET, J. (2010). The anatomy of a 'suture zone' in amazonian butterflies: a coalescent-based test for vicariant geographic divergence and speciation. *Molecular Ecology*, 19(19):4283–4301.

[15] Ebdon, S., Laetsch, D. R., Dapporto, L., Hayward, A., Ritchie, M. G., Dincă, V., Vila, R., and Lohse, K. (2020). The pleistocene species pump past its prime: evidence from european butterfly sister species. *bioRxiv*.

[16] Ewing, G. B. and Jensen, J. D. (2016). The consequences of not accounting for background selection in demographic inference. *Molecular Ecology*, 25(1):135–141.

[17] Feliner, G. N. (2011). Southern European glacial refugia: A tale of tales. *Taxon*, 60(2):365–372.

[18] Gattepaille, L. M., Jakobsson, M., and Blum, M. G. B. (2013). Inferring population size changes with sequence and SNP data: lessons from human bottlenecks. *Heredity*, 110(5):409–19.

[19] Gaume, L., Matile-Ferrero, D., and McKey, D. (2000). Colony foundation and acquisition of coccoid trophobionts by aphomomyrmex afer (formicinae): co-dispersal of queens and phoretic mealybugs in an ant-plant-homopteran mutualism? *Insectes soc*, 47:84—-91.

[20] Gutenkunst, R. N., Hernandez, R. D., Williamson, S. H., Bustamante, C. D., and Stephan, W. (2009). Inferring the Joint Demographic History of Multiple Populations from Multidimensional SNP Frequency Data. *PLoS Genetics*, 5(10):e1000695.

[21] Hall, A. R., Ashby, B., Bascompte, J., and King, K. C. (2020). Measuring coevolutionary dynamics in species-rich communities. *Trends in Ecology Evolution*, 35(6):539–550.

[22] Hayward, A. and Stone, G. N. (2006). Comparative phylogeography across two trophic levels: the oak gall wasp Andricus kollari and its chalcid parasitoid Megastigmus stigmatizans. *Molecular Ecology*, 15(2):479–489.

[23] Hearn, J., Stone, G. N., Bunnefeld, L., Nicholls, J. A., Barton, N. H., and Lohse, K. (2014). Likelihood-based inference of population history from low-coverage de novo genome assemblies. *Molecular Ecology*, 23(1):198–211.

[24] Hewitt, G. (2000). The genetic legacy of the Quaternary ice ages. *Nature*, 405(6789):907–913.

[25] Hewitt, G. M. (1996). Some genetic consequences of ice ages, and their role in divergence and speciation. *Biological journal of the Linnean Society*, 58(3):247–276.

[26] Hickerson, M., Carstens, B., Cavender-Bares, J., Crandall, K., Graham, C., Johnson, J., Rissler, L., Victoriano, P., and Yoder, A. (2010). Phylogeography's past, present, and future: 10 years after avise, 2000. *Molecular Phylogenetics and Evolution*, 54(1):291–301.

[27] Hofreiter, M. and Stewart, J. (2009). Ecological Change, Range Fluctuations and Population Dynamics during the Pleistocene. *Current Biology*, 19(14):R584–R594.

[28] Janzen, D. (1985). On ecological fitting. *Oikos*, 45(3):308–310.

[29] Keightley, P. D., Trivedi, U., Thomson, M., Oliver, F., Kumar, S., and Blaxter, M. L. (2009). Analysis of the genome sequences of three Drosophila melanogaster spontaneous mutation accumulation lines. *Genome research*, 19(7):1195–201.

[30] Kelleher, J., Etheridge, A. M., and McVean, G. (2016). Efficient Coalescent Simulation and Genealogical Analysis for Large Sample Sizes. *PLoS Computational Biology*, 12(5):1–22.

[31] Kelleher, J., Wong, Y., Wohns, A. W., Fadil, C., Albers, P. K., and McVean, G. (2019). Inferring whole-genome histories in large population dataset. *Nature Genetics*, 51(9):1330–1338.

[32] Leaché, A. D., Crews, S. C., and Hickerson, M. J. (2007). Two waves of diversification in mammals and reptiles of baja california revealed by hierarchical bayesian analysis. *Biology Letters*, 3(6):646–650.

[33] Li, H. and Durbin, R. (2009). Fast and accurate short read alignment with Burrows-Wheeler transform. *Bioinformatics*, 25(14):1754–1760.

[34] Li, H. and Durbin, R. (2011). Inference of human population history from individual whole-genome sequences. *Nature*, 475(7357):493–496.

[35] Li, H., Handsaker, B., Wysoker, A., Fennell, T., Ruan, J., Homer, N., Marth, G., Abecasis, G., and Durbin, R. (2009). The Sequence Alignment/Map format and SAMtools. *Bioinformatics*, 25(16):2078–2079.

[36] Li, W. H. and Graur, D. (1991). *Fundamentals of Molecular Evolution*. Sunderland, MA: Sinauer Associates.

[37] Lohse, K., Barton, N., Melika, G., and Stone, G. (2012). A likelihood-based comparison of population histories in a parasitoid guild. *Molecular Ecology*, 21:4605–4617.

[38] Lohse, K., Harrison, R. J., and Barton, N. H. (2011). A general method for calculating likelihoods under the coalescent process. *Genetics*, 189(3):977–87.

[39] Lohse, K., Sharanowski, B., and Stone, G. N. (2010). Quantifying the pleistocene history of the oak gall parasitoid Cecidostiba fungosa using twenty intron loci. *Evolution*, 64(9):2664–2681.

[40] Mackintosh, A., Laetsch, D. R., Hayward, A., Charlesworth, B., Waterfall, M., Vila, R., and Lohse, K. (2019). The determinants of genetic diversity in butterflies. *Nature Genetics*, 10(1):3466.

[41] MJ, W. (2007). The co-evolutionary genetics of ecological communities. *Nat Rev Genet*, 8(3):185–95.

[42] Nei, M. (1972). Genetic distance between populations. *The American Naturalist*, 106(949):283–292.

[43] Nicholls, J. A., Challis, R. J., Mutun, S., and Stone, G. N. (2012). Mitochondrial barcodes are diagnostic of shared refugia but not species in hybridizing oak gallwasps. *Molecular Ecology*, 21(16):4051–4062.

[44] Nicholls, J. A., Preuss, S., Hayward, A., Melika, G., Csóka, G., Nieves-Aldrey, J.-L., Askew, R. R., Tavakoli, M., Schönrogge, K., and Stone, G. N. (2010). Concordant phylogeography and cryptic speciation in two Western Palaearctic oak gall parasitoid species complexes. *Molecular Ecology*, 19(3):592–609.

[45] Nicholls, J. A., Schönrogge, K., Preuss, S., and Stone, G. N. (2018). Partitioning of herbivore hosts across time and food plants promotes diversification in the megastigmus dorsalis oak gall parasitoid complex. *Ecology and Evolution*, 8(2):1300–1315.

[46] Östergård, H. and Ehrlén, J. (2005). Among population variation in specialist and generalist seed predation - the importance of host plant distribution, alternative hosts and environmental variation. *Oikos*, 111(1):39–46.

[47] Papadopoulou, A. and Knowles, L. L. (2016). Toward a paradigm shift in comparative phylogeography driven by trait-based hypotheses. *Proceedings of the National Academy of Sciences*, 113(29):8018–8024.

[48] Petit, R. J., Brewer, S., Bordács, S., Burg, K., Cheddadi, R., Coart, E., Cottrell, J., Csaikl, U. M., van Dam, B., Deans, J. D., Espinel, S., Fineschi, S., Finkeldey, R., Glaz, I., Goicoechea, P. G., Jensen, J. S., König, A. O., Lowe, A. J., Madsen, S. F., Mátyás, G., Munro, R. C., Popescu, F., Slade, D., Tabbener, H., de Vries, S. G., Ziegenhagen, B., de Beaulieu, J.-L., and Kremer, A. (2002). Identification of refugia

and post-glacial colonisation routes of European white oaks based on chloroplast DNA and fossil pollen evidence. *Forest Ecology and Management*, 156(1-3):49–74.

[49] Rand, T. A. and Tscharntke, T. (2007). Contrasting effects of natural habitat loss on generalist and specialist aphid natural enemies. *Oikos*, 116(8):1353–1362.

[50] Ricklefs, R. E. (2015). Intrinsic dynamics of the regional community. *Ecology Letters*, 18(6):497–503.

[51] Rokas, A., Atkinson, R. J., Brown, G. S., West, S. A., and Stone, G. N. (2001). Understanding patterns of genetic diversity in the oak gallwasp Biorhiza pallida: demographic history or a Wolbachia selective sweep? *Heredity*, 87(3):294–304.

[52] Rokas, A., Atkinson, R. J., Webster, L., Csoka, G., and Stone, G. N. (2003). Out of Anatolia: longitudinal gradients in genetic diversity support an eastern origin for a circum-Mediterranean oak gallwasp Andricus quercustozae. *Molecular Ecology*, 12(8):2153–2174.

[53] Satler, J. D. and Carstens, B. C. (2017). Do ecological communities disperse across biogeographic barriers as a unit? *Molecular Ecology*, 26(13):3533–3545.

[54] Schrider, D. R., Shanku, A. G., and Kern, A. D. (2016). Effects of linked selective sweeps on demographic inference and model selection. *Genetics*, 204(3):1207–1223.

[Smith et al.] Smith, B., McCormack, J., Cuervo, A., Hickerson, M., Aleixo, A., Cadena, C., Pérez-Emán, J., Burney, C., Xie, X., Harvey, M., Faircloth, B., Glenn, T., Derryberry, E., Prejean, J., Fields, S., and Brumfield, R. The drivers of tropical speciation. *Nature*, 515(7527).

[56] Smith, J. M. and Haigh, J. (1974). The hitch-hiking effect of a favourable gene. *Genet. Res., Camb*, 23:23–35.

[57] Speidel, L., Forest, M., Shi, S., and Myers, S. R. (2019). A method for genome-wide genealogy estimation for thousands of samples. *Nature Genetics*, 51(9):1321–1329.

[58] Stanke, M. and Morgenstern, B. (2005). AUGUSTUS: a web server for gene prediction in eukaryotes that allows user-defined constraints. *Nucleic acids research*, 33(Web Server issue):W465–7.

[59] Stone, G., Lohse, K., Nicholls, J., Fuentes-Utrilla, P., Sinclair, F., Schönrogge, K., Csóka, G., Melika, G., Nieves-Aldrey, J.-L., Pujade-Villar, J., Tavakoli, M., Askew, R., and Hickerson, M. (2012). Reconstructing Community Assembly in Time and Space Reveals Enemy Escape in a Western Palearctic Insect Community. *Current Biology*, 22(6):532–537.

[60] Stone, G. N., Challis, R. J., Atkinson, R. J., Csóka, G., Hayward, A., Melika, G., Mutun, S., Preuss, S., Rokas, A., Sadeghi, E., and Schönrogge, K. (2007). The phylogeographical clade trade: tracing the impact of human-mediated dispersal on the colonization of northern Europe by the oak gallwasp Andricus kollari. *Molecular Ecology*, 16(13):2768–2781.

[61] Stone, G. N., Schönrogge, K., Atkinson, R. J., Bellido, D., and Pujade-Villar, J. (2002). The population biology of oak gall wasps (Hymenoptera : Cynipidae). *Annual Review of Entomology*, 47(1):633–668.

[62] Stone, G. N., White, S. C., Csóka, G., Melika, G., Mutun, S., Pénzes, Z., Sadeghi, S. E., Schönrogge, K., Tavakoli, M., and Nicholls, J. A. (2017). Tournament ABC analysis of the western Palaearctic population history of an oak gall wasp, Synergus umbraculus. *Molecular Ecology*, 26(23):6685–6703.

[63] Tison, J.-L., Edmark, V. N., Sandoval-Castellanos, E., Van Dyck, H., Tammaru, T., Välimäki, P., Dalén, L., and Gotthard, K. (2014). Signature of post-glacial expansion and genetic structure at the northern range limit of the speckled wood butterfly. *Biological Journal of the Linnean Society*, 113(1):136–148.

[64] Van der Auwera, G. A., Carneiro, M. O., Hartl, C., Poplin, R., del Angel, G., Levy-Moonshine, A., Jordan, T., Shakir, K., Roazen, D., Thibault, J., Banks, E., Garimella, K. V., Altshuler, D., Gabriel, S., and DePristo, M. A. (2013). From FastQ Data to High-Confidence Variant Calls: The Genome Analysis Toolkit Best Practices Pipeline. *Current Protocols in Bioinformatics*, 43(1):11.10.1–11.10.33.

[65] Vitales, D., García-Fernández, A., Garnatje, T., Pellicer, J., and Vallès, J. (2016). Phylogeographic insights of the lowland species cheirolophus sempervirens in the southwestern iberian peninsula. *Journal of Systematics and Evolution*, 54(1):65–74.

[66] Wakeley, J. (2008). *Coalescent Theory: An Introduction*. W. H. Freeman.

[67] Wall, J. D. (2003). Estimating ancestral population sizes and divergence times. *Genetics*, 163(1):395–404.

[68] Wan, T., Oaks, J. R., Jiang, X.-L., Huang, H., and Knowles, L. L. (2021). Differences in quaternary co-divergence reveals community-wide diversification in the mountains of southwest china varied among species. *Proceedings of the Royal Society B: Biological Sciences*, 288(1942):20202567.

[69] Weinersmith, K. L., Liu, S. M., Forbes, A. A., and Egan, S. P. (2017). Tales from the crypt: a parasitoid manipulates the behaviour of its parasite host. *Proceedings of the Royal Society B: Biological Sciences*, 284(1847):20162365.

[70] Wolfram Research, I. (2016). Mathematica.

[71] Xue, A. T. and Hickerson, M. J. (2020). Comparative phylogeographic inference with genome-wide data from aggregated population pairs. *Evolution*, 74(5):808–830.

Data Accessibility

- Raw reads have been deposited in the European Nucleotide Archive (ENA) (ERP023079) and the SRA (PRJEB20883)
- Genome assemblies are deposited in the ENA (PRJEB27189 and ERP109243)
- *Mathematica* notebook and blockwise data are available as Supporting Information

Author Contributions

KL and GS designed the project; WW analysed the sequence data with contributions from KL; all authors wrote the manuscript.

Supplementary information

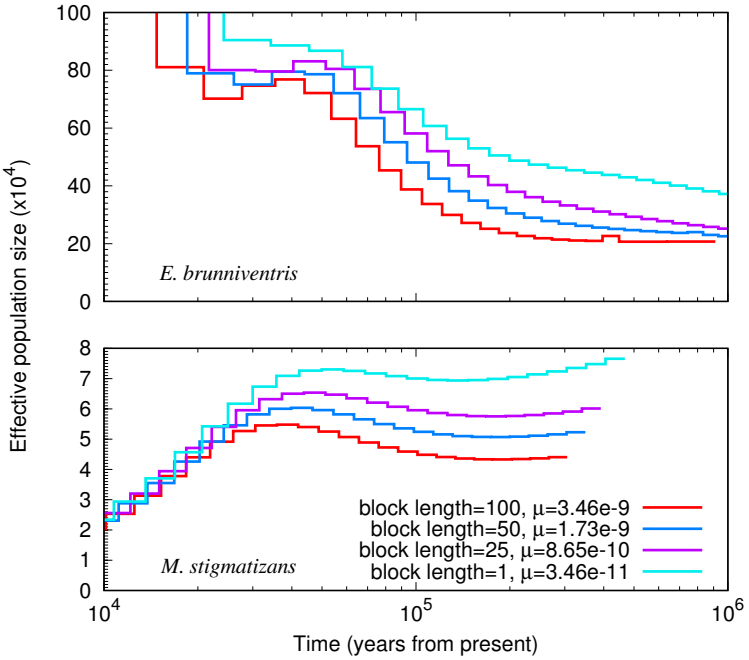

Figure S1: N_e trajectories inferred by PSMC using different block lengths for *E. brunniventris* and *M. stigmatizans*. The mutation rate is adjusted accordingly for each block length.

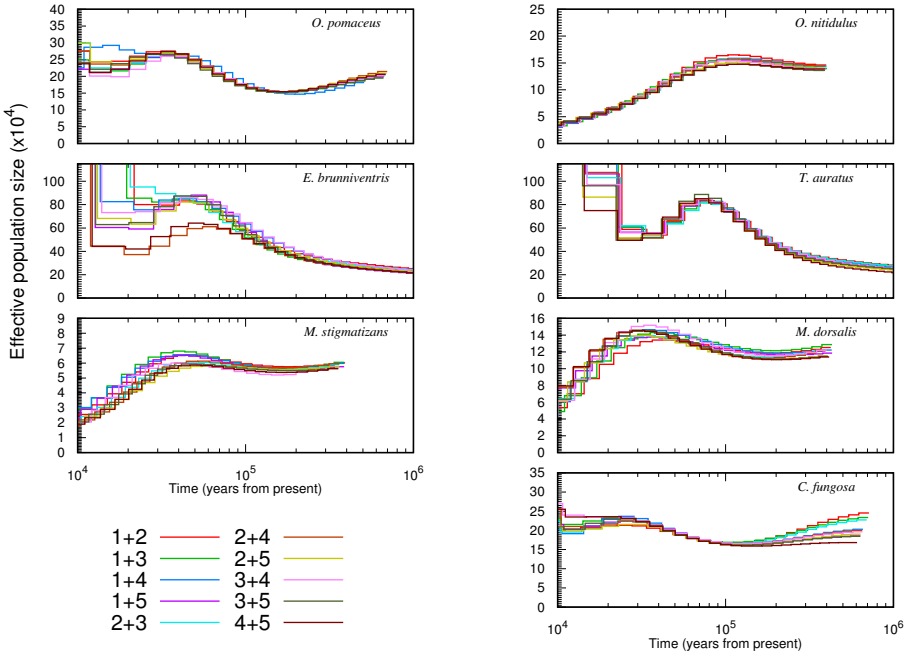

Figure S2: N_e trajectories inferred by PSMC for all pairwise combinations of the five Iberian haploid males of each species. Individuals 1 and 2 for each species correspond to the focal pair in figures 1 2.

Table S1: Sampling locations and gallwasp hosts of parasitoid individuals used for whole genome sequencing. *: The two focal Iberian individuals used for PSMC analysis †: Individuals previously analysed by Bunnefeld et al. (9)

Species	Host range	Individual	Host species	Locality country	Locality region	Locality name	Lat	Long
T. auratus	44	Taur1387	*Andricus quercustozae*	Portugal		Paradella		
		Taur435*	*Biorhiza pallida*	Spain	Cádiz	San Pablo	36.50	-5.37
		Taur436	*Biorhiza pallida*	Spain	Cádiz	San Pablo	36.50	-5.37
		Taur438*	*Biorhiza pallida*	Portugal	Bragança	Vale de Lamas	41.48	-6.5
		Taur409†	*Andricus quercustozae*	Spain	Madrid	El Escorial	40.58	-4.13
		Taur130†	*Cynips quercusfolii*	Hungary		Jaszbereny	47.50	19.92
M. stigmatizans	21	Msti297	*Andricus kollari*	Spain	Salamanca	Horcajo	40.64	-5.41
		Msti393	*Andricus kollari*	Spain	Salamanca	Fresnedoso & Sorihuela		
		Msti311*	*Andricus kollari*	Spain	Salamanca	Horcajo	40.64	-5.41
		Msti004*	*Andricus quercustozae*	Spain		Predo del Rey		
		Msti395†	*Andricus kollari*	Spain	Salamanca	Horcajo	40.64	-5.41
		Msti553B†	*Andricus kollari*	Hungary				
M. dorsalis	65	Mdor2928	*Andricus quercustozae*	Portugal		Gimonde		
		Mdor1555*	*Andricus quercustozae*	Spain	Avila	Puerto de Villatoro	40.55	-5.17
		Mdor1429	*Andricus quercustozae*	Portugal		Outeiro		
		Mdor1348B*†	*Andricus kollari*	Spain	Salamanca	Horcajo	40.64	-5.41
		Mdor1457B†	*Andricus kollari*	Spain	Madrid	El Escorial	40.58	-4.13
		Mdor1448†	*Aphelonyx cerricola*	Hungary		Godollo	47.60	19.38
O. nitidulus	54	Onit388	*Andricus kollari*	Spain	Madrid	El Escorial	40.58	-4.13
		Onit171*	*Andricus kollari*	Portugal		Lagarelhos		
		Onit793*	*Andricus kollari*	Spain	Avila	Lanzahita		
		Onit1085	*Andricus kollari*	Portugal		Lagarelhos		
		Onit386B†	*Andricus kollari*	Spain	Avila	Lanzahita		
		Onit1633†	*Andricus lucidus*	Hungary		Godollo	47.6	19.38
O. pomaceus	87	Opom674	*Cynips quercus*	Spain	Salamanca	Fresnedoso & Sorihuela		
		Opom686	*Cynips quercus*	Spain	Salamanca	Fresnedoso & Sorihuela		
		Opom314*	*Cynips quercus*	Spain	Salamanca	Fresnedoso & Sorihuela		
		Opom344*†	*Andricus grosulariae*	Spain	Caceres	Aldeanueva del Camino	40.26	-5.93
		Opom66	*Cynips quercus*	Spain	Avila	La Canada		
		Opom688†	*Andricus grossulariae*	Hungary		Mátrafüred	47.83	19.97
E. brunniventris	89	Ebru1130*	*Trygonaspis synaspis*	Spain		Valpallego		
		Ebru1406	*Andricus quercustozae*	Spain	Madrid	Cotes de Monterey		
		Ebru1413	*Andricus curvator*	Spain	Segovia	El Negredo		
		Ebru719*†	*Andricus kollari*	Spain		Navacerrade	40.73	-4.00
		Ebru1132†	*Andricus kollari*	Spain		Nuevo Baztan	40.37	-3.24
		Ebru1927†	*Aphelonyx cerricola*	Hungary		Márkó	47.12	17.81
C. fungosa	59	Cfun135*†	*Andricus quercustozae*	Spain	Avila	Puerto de Villatoro	40.55	-5.17
		Cfun139*	*Andricus quercustozae*	Spain	Avila	Puerto de Villatoro	40.55	-5.17
		Cfun3528		Spain				
		Cfun142†	*Andricus quercustozae*	Spain	Madrid	El Escorial	40.58	-4.13
		Cfun143	*Andricus quercustozae*	Spain	Salamanca	Fresnedoso & Sorihuela		
		Cfun71†	*Andricus caputmedusae*	Hungary		Mátrafüred	47.83	19.97

Table S2: Simulation investigation of recombination bias in the likelihood method. When varying λ and block length, we assumed a recombination rate of 2.3×10^{-9}. The comparison of genic and intergenic regions is performed on real data

Independent parameter	θ	λ	T
recombination rate (/bp/generation)			
input parameters:	1.5	0.5	0.5
0	1.509	0.480	0.492
3.46×10^{-11}	1.520	0.498	0.500
2.3×10^{-10}	1.518	0.502	0.470
7.3×10^{-10}	1.525	0.506	0.425
2.3×10^{-9}	1.457	0.497	0.281
7.3×10^{-9}	1.195	0.420	0.100
2.3×10^{-8}	1.885	0.668	0.007
λ			
input parameters:	1.0		1.0
0.1	1.130	0.084	0.864
0.25	1.089	0.292	0.809
0.5	1.052	0.622	0.662
0.75	0.912	0.794	0.100
1	1.067	1.307	1.275
1.25	1.049	1.617	1.165
1.5	1.046	1.909	1.067
2	1.032	2.636	1.077
2.5	1.025	3.289	1.055
genomic regions of *O. nitidulus*			
whole genome	0.381	0.245	0.683
intergenic	0.401	0.265	0.591
genic	0.359	0.231	0.903

Table S3: Assembly summaries. N50: 50% of the assembly is contained in contigs of length equal to or greater than this value. CEGMA (Core Eukaryotic Genes Mapping Approach): full or partial presence of a core set of eukaryotic genes. r: recombination rate per base pair per generation estimated by Bunnefeld et al. (9).

Species	**Assembler**	**N50**	**Assembly size >200 bases**	**Number of contigs >200 bases**	**CEGMA % complete**	**CEGMA % partial**	**Median coverage per individual**	**Total length (blocks)**	**Total length (PSMC)**	r
T. auratus	SPAdes	10,570	397,870,892	100,431	91.53	97.18	6.55	146,116,456	201,729,257	1.7×10^{-9}
M. stigmatizans	MaSuRCA	9,143	577,876,374	182,922	93.55	97.98	4.25	103,668,048	270,416,674	1.3×10^{-8}
M. dorsalis	MaSuRCA	18,748	589,959,111	148,702	95.16	97.58	4.25	92,678,220	369,548,731	3.0×10^{-9}
O. nitidulus	SPAdes	22,984	259,884,369	37,082	95.16	99.19	6.29	112,143,992	175,944,993	2.3×10^{-9}
O. pomaceus	SPAdes	31,593	263,296,421	43,391	93.15	97.98	6.40	150,762,088	187,178,948	3.9×10^{-9}
E. brunniventris	SPAdes	3,829	393,847,642	200,270	90.73	98.79	6.16	53,696,839	167,341,525	3.1×10^{-9}
C. fungosa	SPAdes	8,7417	182,108,758	18,121	93.55	95.97	8.95	122,999,890	160,721,439	3.6×10^{-9}

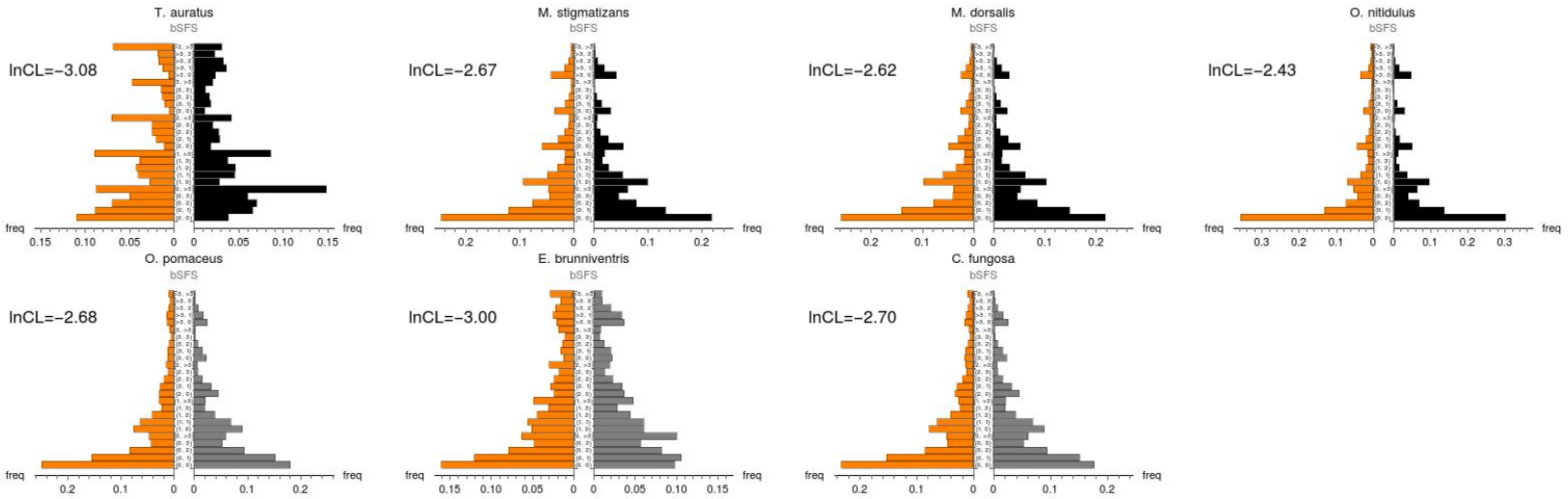

Figure S3: Goodness of fit of the best fitting demographic histories for seven species of parasitoids. The observed frequencies of blockwise configurations defined via the folded SFS are shown in orange (left). The expected frequency under the best fitting history is shown on the right for four species fitting a step change model (top, black) and three species for which a constant N_e could not be rejected (bottom, gray). For a sample of $n = 5$ the folded SFS has two entries $j_{2,3}, j_{1,4}$. The log composite likelihood, $lnCL$ (per block), a measure of absolute goodness of fit of the data to the inferred model, is shown for each species.